The Plant Cell, Vol. 18, 502–514, February 2006, www.plantcell.org 

# Host-Mediated Phosphorylation of Type III Effector AvrPto Promotes *Pseudomonas* Virulence and Avirulence in Tomato [W]

**Jeffrey C. Anderson,[a,b] Pete E. Pascuzzi,[a,b] Fangming Xiao,[b] Guido Sessa,[c] and Gregory B. Martin[b,d,1]**

[a] Department of Molecular Biology and Genetics, Cornell University, Ithaca, New York 14853-2703
[b] Boyce Thompson Institute for Plant Research, Ithaca, New York 14853-1801
[c] Department of Plant Sciences, Tel Aviv University, Tel Aviv, Israel 69978
[d] Department of Plant Pathology, Cornell University, Ithaca, New York 14853-4203

**The AvrPto protein from *Pseudomonas syringae* pv *tomato* is delivered into plant cells by the bacterial type III secretion system, where it either promotes host susceptibility or, in tomato plants expressing the Pto kinase, elicits disease resistance. Using two-dimensional gel electrophoresis, we obtained evidence that AvrPto is phosphorylated when expressed in plant leaves. In vitro phosphorylation of AvrPto by plant extracts occurs independently of Pto and is due to a kinase activity that is conserved in tomato (*Solanum lycopersicum*), tobacco (*Nicotiana tabacum*), and *Arabidopsis thaliana*. Three Ser residues clustered in the C-terminal 18 amino acids of AvrPto were identified in vitro as putative phosphorylation sites, and one site at S149 was directly confirmed as an in vivo phosphorylation site by mass spectrometry. Substitution of Ala for S149 significantly decreased the ability of AvrPto to enhance disease symptoms and promote growth of *P. s. tomato* in susceptible tomato leaves. In addition, S149A significantly decreased the avirulence activity of AvrPto in resistant tomato plants. Our observations support a model in which AvrPto has evolved to mimic a substrate of a highly conserved plant kinase to enhance its virulence activity. Furthermore, residues of AvrPto that promote virulence are also monitored by plant defenses.**

## INTRODUCTION

A successful strategy used by many bacterial pathogens of both plants and animals is to use their type III secretion system to inject into the host cell an array of effector proteins that promote disease by altering host cellular activities (Buttner and Bonas, 2003). *Pseudomonas syringae* pv *tomato* (*Pst*), the causative agent of bacterial speck disease in tomato (*Solanum lycopersicum*), requires the type III secretion of effector proteins for successful growth in the host (Alfano and Collmer, 2004). Recent studies, benefiting from the sequencing of the *Pst* strain DC3000 genome, have identified >20 effector proteins that are likely delivered by *Pst* DC3000 into the plant cell (Collmer et al., 2002). The combined activity of an unknown number of these effectors within the host is critical for successful infection and growth of the pathogen, and intense study of many individual effectors is currently underway (Alfano and Collmer, 2004).

An important component of disease resistance in plants is the gene-for-gene interaction, in which a plant resistance (R) protein recognizes a pathogen avirulence (Avr) protein (Martin et al., 2003). This recognition results in the induction of defenses, including cell wall thickening, production of reactive oxygen species, increased defense gene expression, and localized programmed cell death known as the hypersensitive response. In tomato, the R protein Pto is a Ser/Thr kinase that provides resistance against *Pst* strains expressing *avrPto* or *avrPtoB* (Pedley and Martin, 2003). AvrPto is a type III effector that is secreted into the host cell. In resistant plants, AvrPto is likely recognized through a direct interaction with Pto. Another tomato protein, Prf, which contains a nucleotide binding site and a region of Leu-rich repeats, is also required for Pto-mediated recognition of AvrPto (Salmeron et al., 1996). Prf likely acts either directly with or downstream of the Pto kinase, although its role in resistance is unknown.

In addition to its role in eliciting resistance, several lines of evidence suggest that AvrPto also functions in susceptible plants to promote virulence of *Pst*. Introduction of AvrPto into a *Pst* strain lacking AvrPto enhances bacterial growth and visible disease symptoms on susceptible tomato plants (Chang et al., 2000; Shan et al., 2000a). Also, overexpression of AvrPto in *Arabidopsis thaliana* suppresses the expression of cell wall–associated defense genes, inhibits callose deposition in response to *Pst* infection, and increases bacterial growth (Hauck et al., 2003). A recent report also indicates that AvrPto can suppress cell death in response to nonhost pathogens (Kang et al., 2004). Although the molecular mechanisms underlying these observations are unknown, the occurrence of virulence-associated phenotypes for AvrPto in diverse plant species suggests that some host targets of AvrPto might be conserved. Several putative host targets of AvrPto have been identified from a yeast two-hybrid screen, including a stress-responsive protein and two Rab GTPases (Bogdanove and Martin, 2000). Whether or not these interactions occur in vivo, and the possible functional contribution of each

[1] To whom correspondence should be addressed. E-mail gbm7@cornell.edu; fax 607-255-6695.
The author responsible for distribution of materials integral to the findings presented in this article in accordance with the policy described in the Instructions for Authors (www.plantcell.org) is: Gregory B. Martin (gbm7@cornell.edu).
[W] Online version contains Web-only data.
Article, publication date, and citation information can be found at www.plantcell.org/cgi/doi/10.1105/tpc.105.036590.

interaction to the virulence phenotypes mentioned above, is unknown.

AvrPto is an 18-kD protein with a central core that adopts a three-α-helix bundle structure (Wulf et al., 2004). Approximately 30 amino acids at both the N and C termini are unstructured and flexible in solution. Although AvrPto has no overall sequence homology to any known proteins, different functional properties have been attributed to each of the structurally distinct regions of the protein. Amino acids required for interaction with Pto reside in a large Ω-loop, named the GINP loop, located within the structured core (Wulf et al., 2004). Mutation of residues within the GINP loop disrupts AvrPto interaction with Pto in a yeast two-hybrid system and abolishes Pto-mediated resistance in tomato leaves (Shan et al., 2000a; Wulf et al., 2004). The N terminus of AvrPto contains a myristoylation motif that localizes AvrPto to the plant plasma membrane and is required for both avirulence and virulence functions of the protein (Shan et al., 2000b; Thara et al., 2004). Finally, deletions of the AvrPto C terminus do not disrupt the interaction with Pto in a yeast two-hybrid assay or Pto-mediated recognition of AvrPto transiently expressed in plants (Scofield et al., 1996; Tang et al., 1996). Residues within the C terminus are required for recognition of AvrPto in tobacco (*Nicotiana tabacum*) (Shan et al., 2000b), although the *R* gene responsible for this tobacco recognition has yet to be isolated, and contribute slightly to Pto-mediated resistance in tomato (Shan et al., 2000b).

Following delivery into the host, type III effectors function in the host cell to promote disease. One tactic, first discovered with animal pathogens, is for effectors to mimic host proteins either structurally or enzymatically (Stebbins and Galan, 2001). As a result, effectors interact with and modulate the activity of specific targets within the host. For example, the *Yersinia* effector YopH is a Tyr phosphatase that dephosphorylates host proteins involved in immunity signaling pathways, and YopJ is a Cys protease that interacts with and blocks the activation of mitogen-activated protein kinase kinases (Guan and Dixon, 1990; Orth et al., 1999; Navarro et al., 2005). Recently, YopM was found to interact with and also modulate the activity of two distinct protein kinases in mammalian cells (McDonald et al., 2003). A similar paradigm of molecular mimicry is now emerging for type III effectors of plant pathogens (Alfano and Collmer, 2004). For instance, the effector HopPtoD2 is a Tyr phosphatase that suppresses host cell death, and AvrPphB is a Cys protease that specifically cleaves PBS1, a host kinase required for RPS5-mediated resistance in *Arabidopsis* (Bretz et al., 2003; Espinosa et al., 2003; Shao et al., 2003). AvrRpt2 is also a Cys protease that cleaves the membrane-bound host protein RIN4 in *Arabidopsis* (Coaker et al., 2005; Kim et al., 2005).

Some effectors appear to mimic the substrates of eukaryotic enzymes and are, as a result, posttranslationally modified within the host cell. Host-mediated effector modifications identified to date include myristoylation, ubiquitination, and phosphorylation (Kenny et al., 1997; Mudgett and Staskawicz, 1999; Nimchuk et al., 2000; Marcus et al., 2002; Kubori and Galan, 2003). In some cases, important functions have been attributed to these modifications. For example, myristoylation of AvrRpm1 and AvrPto is required for both avirulence and virulence functions of these effectors (Nimchuk et al., 2000; Shan et al., 2000b; Thara et al., 2004). However, the number of effectors that are modified by host enzymes and the functional significance of these modifications are largely unknown. The goal of this work was to investigate if AvrPto undergoes additional posttranslational modifications in plant leaves. Using two-dimensional (2-D) gel electrophoresis, we discovered that AvrPto is phosphorylated in plant cells. We further identified an in vivo phosphorylation site of AvrPto and found that the phosphorylated residue promotes AvrPto-mediated virulence and avirulence of *Pseudomonas* in tomato leaves.

## RESULTS

### AvrPto Undergoes Multiple Posttranslational Modifications in Plant Cells

To identify possible posttranslational modifications of AvrPto, we used *Agrobacterium tumefaciens* to transiently express AvrPto fused to a double hemagluttinin (HA) tag in leaves of *Nicotiana benthamiana*. Leaf protein extracts were prepared and separated using 2-D gel electrophoresis. Immunoblotting with anti-HA antibodies revealed multiple spots at an estimated pI between 4 and 5 and a molecular mass of ~22 kD (Figure 1). These values are close to a predicted pI of 5.1 and size of 20.6 kD for AvrPto-HA. We consistently found that AvrPto separated as

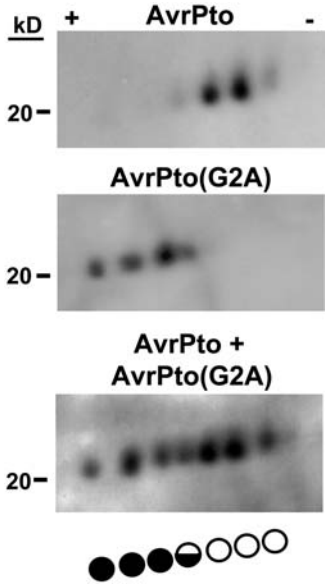


**Figure 1.** AvrPto Undergoes Multiple Modifications in Planta.

AvrPto fused to a double HA tag was expressed in *N. benthamiana* leaves using *Agrobacterium* and separated by 2-D electrophoresis. AvrPto was detected by anti-HA immunoblotting. Shown are blots of wild-type AvrPto (top panel), AvrPto(G2A) (middle panel), or AvrPto and AvrPto(G2A) combined prior to 2-D separation (bottom panel). The basic and acidic ends of the pI gradient are indicated by plus and minus signs, respectively. The diagram below the blots indicates the relative position of AvrPto (white circles) and AvrPto(G2A) (black circles) spots in the pI gradient.

two relatively strong spots flanked by two weaker spots (Figure 1). Occasionally, additional weak spots were detected with a higher pI and smaller mass. The multiple spots suggested that AvrPto is present in the plant cell in at least four different forms that differ both in size and overall charge.

### AvrPto Is Modified in a G2-Dependent Manner When Expressed in Plant Cells

AvrPto contains a predicted N-terminal myristoylation motif that targets the protein to the plant plasma membrane (Shan et al., 2000b). To investigate whether or not the putative modifications of AvrPto are due to myristoylation, we mutated *avrPto* to create a Gly-to-Ala (G2A) substitution at the N terminus and compared the 2-D separation of this altered protein to that of wild-type AvrPto. We found the G2A substitution in AvrPto did not alter the number of spots (Figure 1). However, the entire pattern shifted to a higher pI and smaller size. To confirm this shift, we combined extracts from leaves expressing AvrPto or AvrPto(G2A) prior to 2-D separation and found an increased number of total spots compared with AvrPto or AvrPto(G2A) alone (Figure 1). The overall shift toward a higher pI and smaller molecular mass observed with AvrPto(G2A) is consistent with a loss of an acyl group at the N terminus, as the net positive charge of the protein should increase due to the free amino group at the N terminus. However, the shift in pI due to the G2A substitution is greater than predicted for myristoylation alone. Therefore, it is possible that additional G2-dependent modifications may be contributing to the observed 2-D pattern. Overall, these data indicate that AvrPto undergoes both G2-dependent, and additional G2-independent, modifications.

### AvrPto Is Phosphorylated When Expressed in Plant Cells

The 2-D pattern of AvrPto is suggestive of a phosphorylated protein. To test if AvrPto is phosphorylated, we incubated a protein extract prepared from *N. benthamiana* leaf tissue expressing AvrPto with purified phosphatases PP1 and λ-PPase and separated this extract by 2-D electrophoresis. As a control, we incubated an aliquot of the same extract with PP1, λ-PPase, and inhibitors of both PP1 and λ-PPase. Treatment of the extract with phosphatases resulted in several changes to the AvrPto 2-D pattern (Figure 2A). These changes did not occur upon addition of the phosphatase inhibitors (Figure 2A). In the phosphatase-only treatment, one minor spot disappeared (Figure 2A, arrow 4), and the levels of two major spots were decreased (arrows 2 and 3). In addition, in the phosphatase-only treatment, two weak spots appeared that are not present on the control blot (Figure 2A, arrows 5 and 6). The appearance of spots 5 and 6 occurs in the region where AvrPto(G2A) spots were detected previously (Figure 1) and may be dephosphorylated forms of a small pool of unmyristoylated AvrPto. The sensitivity of the AvrPto 2-D pattern to phosphatase treatment suggests that the observed modifications of AvrPto are due to phosphorylation.

To confirm that AvrPto is phosphorylated in vivo, we used a transient expression system in tomato protoplasts to detect direct labeling of AvrPto in the presence of $^{32}$P-orthophosphate. Leaf protoplasts were transfected with either *35S*:*avrPto-HA* or vector only, incubated with $^{32}$P-orthophosphate, and AvrPto immunoprecipitated with anti-HA antibodies. Autoradiography revealed a single $^{32}$P-labeled band corresponding to AvrPto that is absent in the vector-only lane (Figure 2B). We conclude that AvrPto is modified by phosphorylation in plant cells.

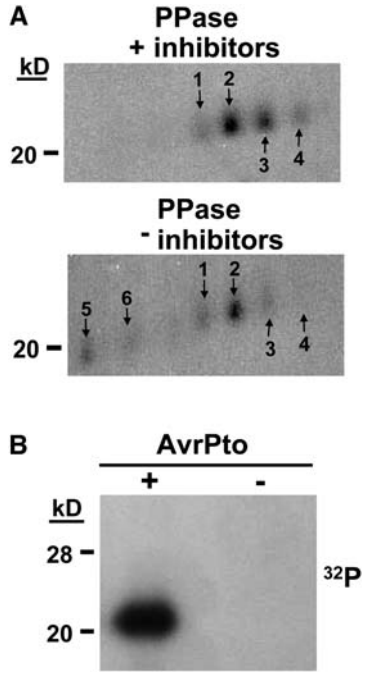


**Figure 2.** AvrPto Is Phosphorylated in Planta.

**(A)** A protein extract from *N. benthamiana* leaves expressing AvrPto-HA was treated with phosphatases PP1 and λ-PPase, in the presence (top panel) or absence (bottom panel) of phosphatase inhibitors, separated by 2-D electrophoresis, and AvrPto detected by anti-HA immunoblotting. Numbered arrows are referred to in the text.

**(B)** Tomato Rio Grande PtoS leaf protoplasts transfected with a *35S*:*avrPto-dHA* vector or empty vector were labeled with $^{32}$P-orthophosphate for 8 h. Protein extracts were prepared and subjected to immunoprecipitation with anti-HA antibody, followed by SDS-PAGE and autoradiography. A single $^{32}$P-labeled band at ~21 kD corresponding to the expected size of AvrPto-dHA was detected from protoplasts expressing AvrPto (+) compared with vector only control (−).

### AvrPto Is Phosphorylated by a *Pto*- and *Prf*-Independent Plant Kinase Activity

To further characterize AvrPto phosphorylation, we developed an in vitro assay to determine if leaf extracts could phosphorylate AvrPto. Recombinant AvrPto fused to the FLAG peptide was expressed in *Escherichia coli* and purified using anti-FLAG resin. Incubating purified AvrPto with [γ-$^{32}$P]ATP and protein extracts from tomato, *N. benthamiana*, *Arabidopsis*, or tobacco leaves resulted in $^{32}$P-labeling of AvrPto (Figure 3A; data not shown). Incorporation of $^{32}$P did not occur in the absence of plant extract or if the extract was boiled prior to the assay (Figure 3A; data not shown). To determine if phosphorylation of AvrPto is dependent on *Pto* or *Prf*, we tested protein extracts from several Rio Grande

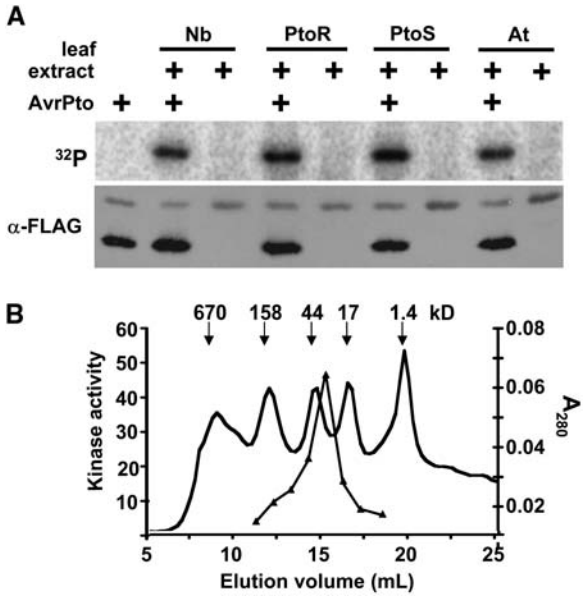


**Figure 3.** AvrPto Is Phosphorylated in Vitro by a 30- to 40-kD Kinase Activity in Leaf Extracts.

**(A)** Recombinant AvrPto with a C-terminal FLAG epitope was expressed in and purified from *E. coli* using α-FLAG resin. AvrPto-FLAG was incubated with leaf protein extracts and [γ-$^{32}$P]ATP and separated by SDS-PAGE. The top panel shows $^{32}$P-detection, and the bottom panel shows anti-FLAG immunoblotting. Lane 1, AvrPto with no leaf extract; lanes 2 to 9, leaf extracts from *N. benthamiana* (Nb), tomato Rio Grande PtoR (RG-PtoR), tomato Rio Grande PtoS (RG-PtoS), and *Arabidopsis* Columbia-0 (Col-0; At) incubated with or without AvrPto. Reactions without AvrPto contained anti-FLAG resin incubated in extracts from *E. coli* expressing empty pFLAG vector.

**(B)** Leaf extracts from tomato Rio Grande PtoS were separated by size exclusion chromatography and each elution fraction tested for kinase activity toward AvrPto as in **(A)**. Graph shows both continuous $A_{280}$ signal and kinase activity toward AvrPto. Units for kinase activity are arbitrary phosphor imager signal counts. The peak of activity was detected in a fraction corresponding to proteins with a size of 30 to 40 kD. The elution positions of standards separated under identical column conditions are indicated.

tomato lines that either contain both *Pto* and *Prf* (RG-PtoR), lack the *Pto* gene (RG-PtoS), or lack a functional *Prf* gene (RG-prf3) for their ability to phosphorylate AvrPto. All of the tomato lines had similar levels of kinase activity toward AvrPto, indicating that Pto and Prf are not required for phosphorylation (Figure 3A; data not shown for RG-prf3). Finally, we were unable to detect phosphorylation of AvrPto by protein extracts from yeast, suggesting that the kinase may be plant specific (data not shown).

### AvrPto Is Phosphorylated by a 30- to 40-kD Kinase in Tomato and Tobacco

Subcellular fractionation of *N. benthamiana* leaf extracts revealed that a majority of the kinase activity toward AvrPto is found in a soluble protein fraction (see Supplemental Figure 1 online). To determine an approximate size of the kinase, we separated an extract of soluble tomato leaf proteins by size exclusion chromatography and assayed each elution fraction for the presence of an activity that could phosphorylate AvrPto in vitro. A peak of activity was observed corresponding to an estimated apparent molecular size of 30 to 40 kD (Figure 3B). A similar size was observed for the kinase activity from tobacco cv W38 leaf extracts (data not shown). We have partially purified the kinase activity from tobacco using several chromatography steps and observe that the activity consistently elutes as a single peak (J.C. Anderson and G.B. Martin, unpublished data). Based on these observations, we believe that AvrPto is a substrate for a 30- to 40-kD kinase activity present in both tomato and tobacco. However, it is possible that AvrPto is phosphorylated by multiple kinases within this size range or that AvrPto is a substrate for additional kinases not detected by our extraction procedures.

### Phosphorylation of AvrPto Occurs on Ser Residues Located at the C Terminus

To identify the residues phosphorylated on AvrPto, we first performed phosphoamino acid analysis on AvrPto phosphorylated in vitro by tomato leaf extracts. Hydrolysis of $^{32}$P-labeled AvrPto to its constituent amino acids followed by thin layer chromatography revealed that only Ser residues are phosphorylated (Figure 4A). The FLAG peptide fused to the C terminus of AvrPto does not contain Ser residues and therefore is not the site

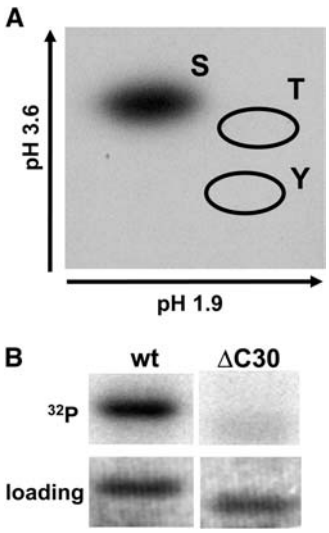


**Figure 4.** In Vitro Phosphorylation Occurs on Ser Residues Located at the C Terminus of AvrPto.

**(A)** AvrPto-FLAG was incubated with tomato RG-PtoS extracts and [γ-$^{32}$P]ATP, hydrolyzed to its constituent amino acids, and separated by 2-D thin layer chromatography. Alignment of the autoradiograph with phosphoamino acid standards (circles) revealed that only Ser residues are phosphorylated in vitro. Identical results were obtained using *N. benthamiana* and *Arabidopsis* extracts (data not shown).

**(B)** Deletion of 30 amino acids from the AvrPto C terminus abolishes in vitro phosphorylation. AvrPto-FLAG or AvrPto(ΔC133-164)-FLAG was phosphorylated in vitro with tomato RG-PtoS extracts and [γ-$^{32}$P]ATP and separated by SDS-PAGE. The top panel is an autoradiograph, and the bottom panel is Coomassie blue staining of the same gel.

of phosphorylation. AvrPto was also phosphorylated only on Ser residues by *N. benthamiana* and *Arabidopsis* leaf protein extracts (data not shown).

AvrPto contains 19 Ser residues that could serve as potential phosphorylation sites. We found that the C-terminal 30 amino acids of AvrPto are enriched for Ser residues, with six Ser residues located in this region. To narrow the list of possible sites, we tested whether deletion of these 30 amino acids (residues 133 to 164) from AvrPto would affect phosphorylation. We expressed full-length AvrPto and AvrPtoΔC30 in *E. coli* as FLAG fusions, purified the proteins, and incubated them with tomato extracts and [$\gamma$-$^{32}$P]ATP. Deletion of 30 amino acids from the C terminus eliminated >95% of the $^{32}$P-incorporation (Figure 4B). These data suggest that phosphorylation of AvrPto occurs on Ser residues located within 30 amino acids from the C terminus.

To identify the AvrPto phosphorylation sites, we substituted Ala residues for each of the six Ser residues at the C terminus individually and assayed for in vitro phosphorylation of the altered proteins using tomato extracts. Ala substitutions at S147, S149, and S153 decreased the level of $^{32}$P-incorporation relative to wild-type AvrPto, whereas Ala substitutions at S136, S156, and S158 had no effect (Figure 5A). None of the individual substitutions completely eliminated $^{32}$P-incorporation, indicating that more than one Ser within this region can be phosphorylated. To generate a phosphorylation-null protein, we substituted Ala for S147, S149, and S153 within the same construct [hereafter referred to as AvrPto(3xS-A)]. Phosphorylation of AvrPto(3xS-A) by tomato, *N. benthamiana*, and *Arabidopsis* extracts was reduced by ~80 to 90% compared with wild-type AvrPto (Figures 5A and 5B). The overall reduction in $^{32}$P-incorporation of AvrPto(3xS-A) is slightly less than the decrease in $^{32}$P-incorporation we observed with AvrPtoΔC30 (>95% reduction; Figure 4B). Therefore, it is possible that other Ser residues at the C terminus, in addition to S147, S149, and S153, are also weakly phosphorylated. Nevertheless, these results suggest that the majority of AvrPto phosphorylation in vitro occurs on Ser residues located in a small region defined by residues S147, S149, and S153 (Figure 5C) and that these residues are phosphorylated by extracts from at least three plant species.

### Identification of S149 as an in Vivo Phosphorylation Site of AvrPto

To determine if AvrPto is phosphorylated in vivo at the sites we mapped in vitro, we compared the 2-D electrophoresis pattern of AvrPto with the Ala-substituted protein AvrPto(3xS-A). Protein extracts were prepared from *N. benthamiana* leaves transiently expressing either AvrPto or AvrPto(3xS-A) and analyzed by 2-D electrophoresis followed by immunoblotting. The 2-D separation of AvrPto(3xS-A) revealed a loss of one minor spot (arrow 4) and the decrease of one major spot (arrow 3) compared with the pattern of AvrPto (Figure 5D). We note that additional weak spots with a higher pI and smaller size are present in Figure 5D that were not present in Figure 1. Detection of these additional spots is likely due to improved immunoblot sensitivity between experiments. The loss of spots in the 2-D pattern of AvrPto(3xS-A) in Figure 5D suggests that residues between S147 and S153 are also phosphorylation sites of AvrPto in vivo.

To identify specific residues that are phosphorylated on AvrPto, we looked for in vivo posttranslational modifications of AvrPto using mass spectrometry. AvrPto-HA was expressed in tomato protoplasts and immunoprecipitated with anti-HA antibodies. As a control, we also expressed and immunoprecipitated AvrPto(ΔC30)-HA in the same manner. SDS-PAGE and Coomassie blue staining of the immunoprecipitated AvrPto-HA revealed an estimated ~25-kD band that was not present in a mock-treated control (Figure 6A; data not shown). As expected, a slightly smaller band was present in the AvrPto(ΔC30) lane (Figure 6A). Protein bands corresponding to AvrPto and AvrPto(ΔC30) were excised from SDS-PAGE gels and digested with trypsin, and the resulting peptides were analyzed by nano-electrospray ionization tandem mass spectrometry (nanoESI-MS/MS). A full MS spectrum scan of the AvrPto digest and subsequent search of the nonredundant National Center for Biotechnology Information (NCBInr) database using Mascot identified 18 ions that matched predicted AvrPto tryptic peptides and unambiguously confirmed the isolated protein as AvrPto (72% sequence coverage; Mowse total score 472) (Figure 6B; data not shown). We were unable to identify any ions in the MS spectrum that matched the predicted mass of a myristoylated or unmyristoylated AvrPto N-terminal peptide, possibly due to the highly hydrophobic nature of the acylated peptide.

A single doubly protonated precursor ion with an observed mass-to-charge value of 688.27 matching a predicted AvrPto phosphopeptide was selected for collision-induced dissociation fragmentation (Figure 6B). The ion mass value corresponds to the AvrPto C-terminal peptide $^{140}$FVATMNPSGSIR$^{151}$, including the addition of 80 D as expected for a single phosphorylation event and an additional 16 D that is often indicative of Met/Cys oxidation. A series of y fragmentation product ions were recorded in MS/MS mode that unambiguously confirmed the precursor ion as the peptide $^{140}$FVATMNPSGSIR$^{151}$, with an additional oxidation of M144 (Figure 6C). To identify the specific residue that is phosphorylated, the MS/MS spectra were analyzed for the neutral loss of phosphoric acid ($H_3PO_4$). Neutral loss of $H_3PO_4$ results in product ions that are 98 D smaller than predicted from the phosphorylated precursor ion (Garcia et al., 2005). In the MS/MS spectrum of ion 688.27, product ions that include S149 are 98 D smaller than predicted. These results directly confirm S149 as an in vivo phosphorylation site of AvrPto. As expected, the 688.27 ion was absent from the mass spectrum of AvrPto(ΔC30) (data not shown).

We did not observe an ion corresponding to an S147- or S153-phosphorylated peptide in the mass spectrum of AvrPto, although an ion matching an unphosphorylated $^{152}$MSTLSPSPYR$^{161}$ peptide was detected (data not shown). In a further attempt to detect additional in vivo phosphorylation sites, we used matrix-assisted laser desorption ionization (MALDI)-MS as an alternative approach. MALDI-MS analysis allowed the detection of an ion that matches the predicted mass of a singly phosphorylated $^{152}$MSTLSPSPYR$^{161}$ peptide (data not shown). However, this observed ion peak also closely matches the predicted mass of a phosphorylated peptide from the N terminus of AvrPto. Given this uncertainty and the lack of MS/MS data, we were unable to unambiguously confirm in vivo phosphorylation at S147 or S153.

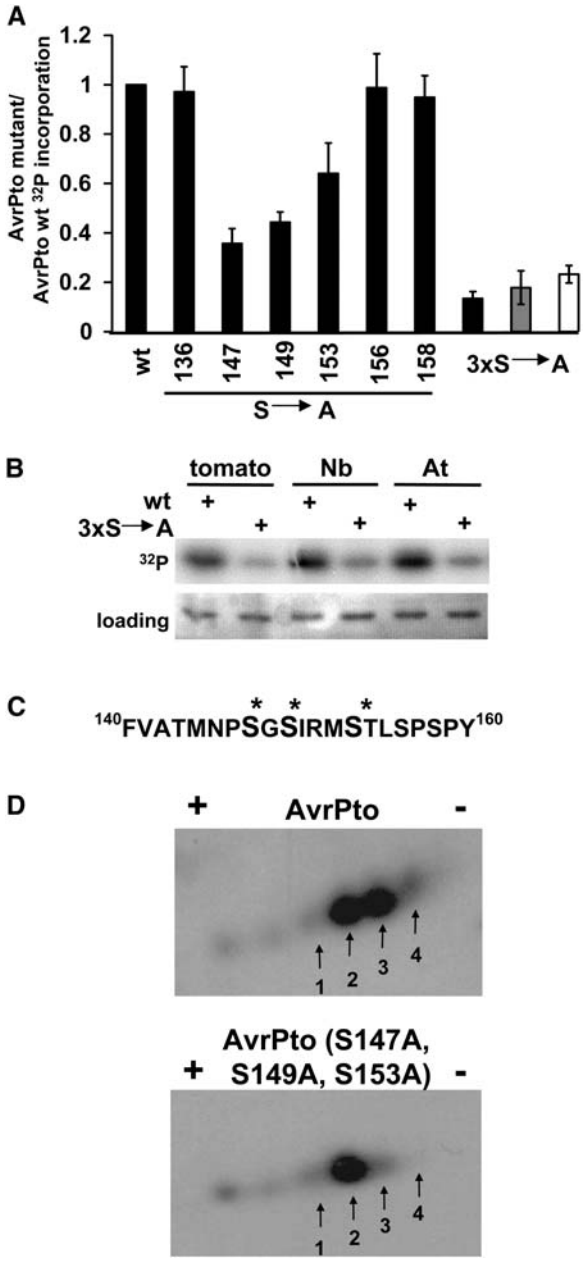


**Figure 5.** Mapping the AvrPto Phosphorylation Sites Using Ala Substitutions.

**(A)** Ser residues at the C terminus of AvrPto were changed to Ala individually or in combination. In vitro kinase reactions were performed with the altered AvrPto proteins using either tomato RG-PtoS (black), *N. benthamiana* (gray), or *Arabidopsis* Col-0 (white) leaf extracts. Graph shows $^{32}$P-incorporation of individual and combined Ser-to-Ala substitutions as a percentage of wild-type AvrPto. Values obtained by the phosphor imager were normalized to levels of protein detected by Coomassie blue staining. Each value represents the mean of at least three independent experiments. Bars indicate ±SE.

**(B)** Recombinant AvrPto-FLAG or AvrPto(S147A, S149A, S153A)-FLAG proteins were incubated with tomato RG-PtoS, *N. benthamiana*, or *Arabidopsis* Col-0 leaf protein extracts and [γ-$^{32}$P]ATP and separated by SDS-PAGE. The top panel shows an autoradiograph, and the bottom panel a Coomassie blue–stained gel.

**(C)** Sequence from the C terminus of AvrPto. Asterisks indicate Ser residues identified as potential phosphorylation sites.

**(D)** AvrPto-dHA or AvrPto(S147A, S149A, S153A)-dHA was expressed using *Agrobacterium* in *N. benthamiana* leaves, separated by 2-D electrophoresis, and detected by anti-HA. The numbered arrows correspond to arrows in Figure 2A and point to one major (arrow 3) and one minor (arrow 4) spot that are decreased or absent, respectively, on the blot of AvrPto(S147A, S149A, S153A) (bottom panel) relative to the blot of AvrPto (top panel).

### The Phosphorylated Residue S149 Contributes to AvrPto Virulence Activity

To test if phosphorylation of S149 contributes to the virulence activity of AvrPto in tomato when expressed and delivered by *Pst*, we vacuum-infiltrated a low inoculum ($10^4$ colony-forming units [cfu]/mL) of *Pst* strain T1 (hereafter referred to as T1) expressing AvrPto with Ala substitutions for S147, S149, or S153 into the leaves of susceptible line RG-prf3 (*Pto*/*Pto prf*/*prf*). As controls, we also infiltrated plants with strains of T1 expressing AvrPto or AvrPto(G2A). As reported elsewhere, we find that T1-AvrPto(G2A) grows to the same level as T1 with empty vector on RG-prf3 plants and causes similar disease symptoms (data not shown; Thara et al., 2004). Because these strains appear equivalent, we chose T1-AvrPto(G2A) for this work rather than T1-empty vector to control for the possibility that AvrPto expression and/or secretion could alter *Pst* growth. As expected, T1-AvrPto caused more severe disease symptoms (Figures 7A to 7C) and grew to levels 20-fold higher than T1-AvrPto(G2A) (Figure 7D; Chang et al., 2000; Thara et al., 2004). Interestingly, we found that T1 expressing either AvrPto(S147A) or AvrPto(S149A) caused disease symptoms that were less severe than T1-AvrPto and grew to levels lower than T1-AvrPto (Figures 7A to 7D). Furthermore, disease symptoms caused by T1-AvrPto(S149A) were less severe than disease caused by T1-AvrPto(S147A) (Figures 7A to 7C). By contrast, T1 expressing AvrPto(S153A) caused disease symptoms indistinguishable from T1-AvPto and grew to similar levels (Figures 7A to 7D). We conclude from these data that both S147 and the phosphorylation site we identified at S149 contribute to AvrPto virulence in tomato.

### The Phosphorylated Residue Ser149 of AvrPto Contributes to *Pto*/*Prf*-Mediated Resistance in Tomato

We next tested if phosphorylation is involved in AvrPto avirulence activity. Leaves of resistant line RG-PtoR (*Pto*/*Pto Prf*/*Prf*) were vacuum infiltrated with a low inoculum ($10^4$ cfu/mL) of T1 expressing AvrPto(S147A), AvrPto(S149A), or AvrPto(S153A) and the controls as described above. As expected, visible disease symptoms did not develop on RG-PtoR plants inoculated with T1-AvrPto, and disease symptoms were present on RG-PtoR plants inoculated with T1-AvrPto(G2A) (data not shown). In addition, T1-AvrPto(G2A) grew to levels 150-fold greater than T1-AvrPto 3 d after infiltration (Figure 7E). We found a low level of speck disease present on RG-PtoR plants infiltrated with either

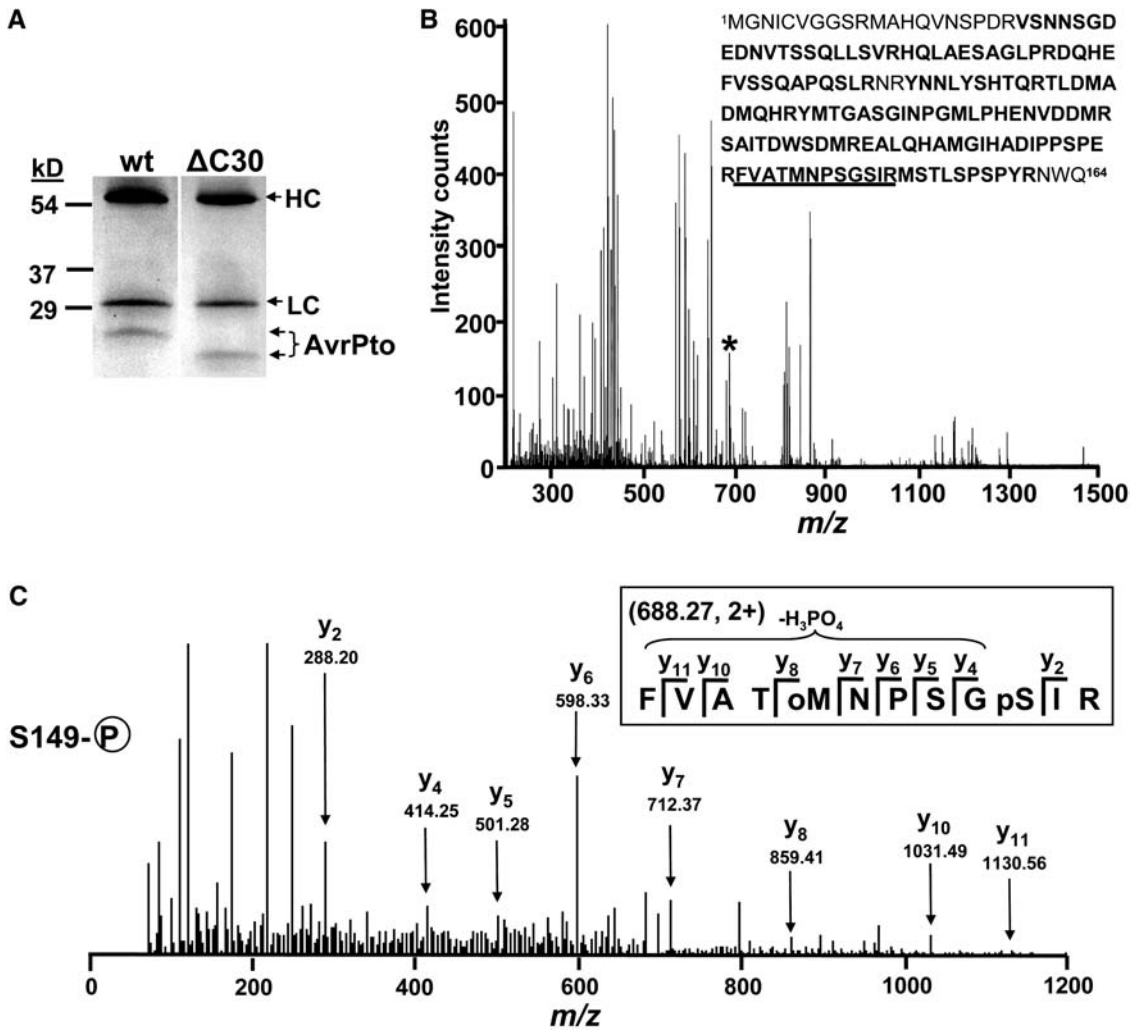


**Figure 6.** Identification of in Vivo Phosphorylation Sites by Mass Spectrometry.

AvrPto was expressed in and immunoprecipitated from RG-prf3 tomato leaf protoplasts and the protein subsequently analyzed by nanoESI-MS/MS to identify phosphorylation sites.

**(A)** SDS-PAGE analysis of AvrPto proteins immunoprecipitated with anti-HA antibody from tomato RG-prf3 leaf protoplasts. Proteins were separated on a 15% gel and stained with colloidal Coomassie blue G 250. Left lane, AvrPto-dHA; right lane, AvrPto(ΔC30)-dHA. Positions of IgG heavy chain (HC) and light chain (LC) are indicated.

**(B)** ESI mass spectrum of AvrPto-dHA digested with trypsin. The ion selected for subsequent MS/MS analysis is designated by an asterisk. Inset is AvrPto sequence with peptides identified by MS in bold. The peptide selected for MS/MS fragmentation is underlined.

**(C)** MS/MS spectrum of precursor ion with observed mass-to-charge ratio ($m/z$) = 688.27 [$(M+2H+O+H_3PO_4)^{2+}$] confirms phosphorylation on Ser149. Inset diagrams the position of identified product ions within the peptide sequence. -$H_3PO_4$ designates product ions that show neutral loss of phosphoric acid. pS indicates phosphorylated Ser. oM indicates oxidized Met.

T1-AvrPto(S147A) or T1-AvrPto(S149A), typically one to two specks per leaflet, whereas no disease was present on plants infiltrated with T1-AvrPto(S153A) (data not shown). Both T1-AvrPto(S147A) and T1-AvrPto(S149A) grew to levels ~10-fold greater than T1-AvrPto by day 3 (Figure 7E). These results agree with a previous report that mutations within the C terminus of AvrPto slightly reduce its avirulence activity in RG-PtoR leaves (Shan et al., 2000b). By contrast, we found that T1-AvrPto(S153A) did not grow to levels greater than T1-AvrPto by day 3 and displayed a trend of decreased growth relative to T1-AvrPto (Figure 7E). We conclude from these data that S147 and S149 contribute to the avirulence activity of AvrPto on RG-PtoR plants. Also, substitution of Ala for S153 may slightly increase rather than decrease the avirulence activity of AvrPto.

We observed no difference in the expression or secretion levels of AvrPto(S147A), AvrPto(S149A), AvrPto(S153A), or AvrPto(G2A) from T1 into hrp-inducing minimal media compared with AvrPto (Figure 7F). Ala substitutions at these residues

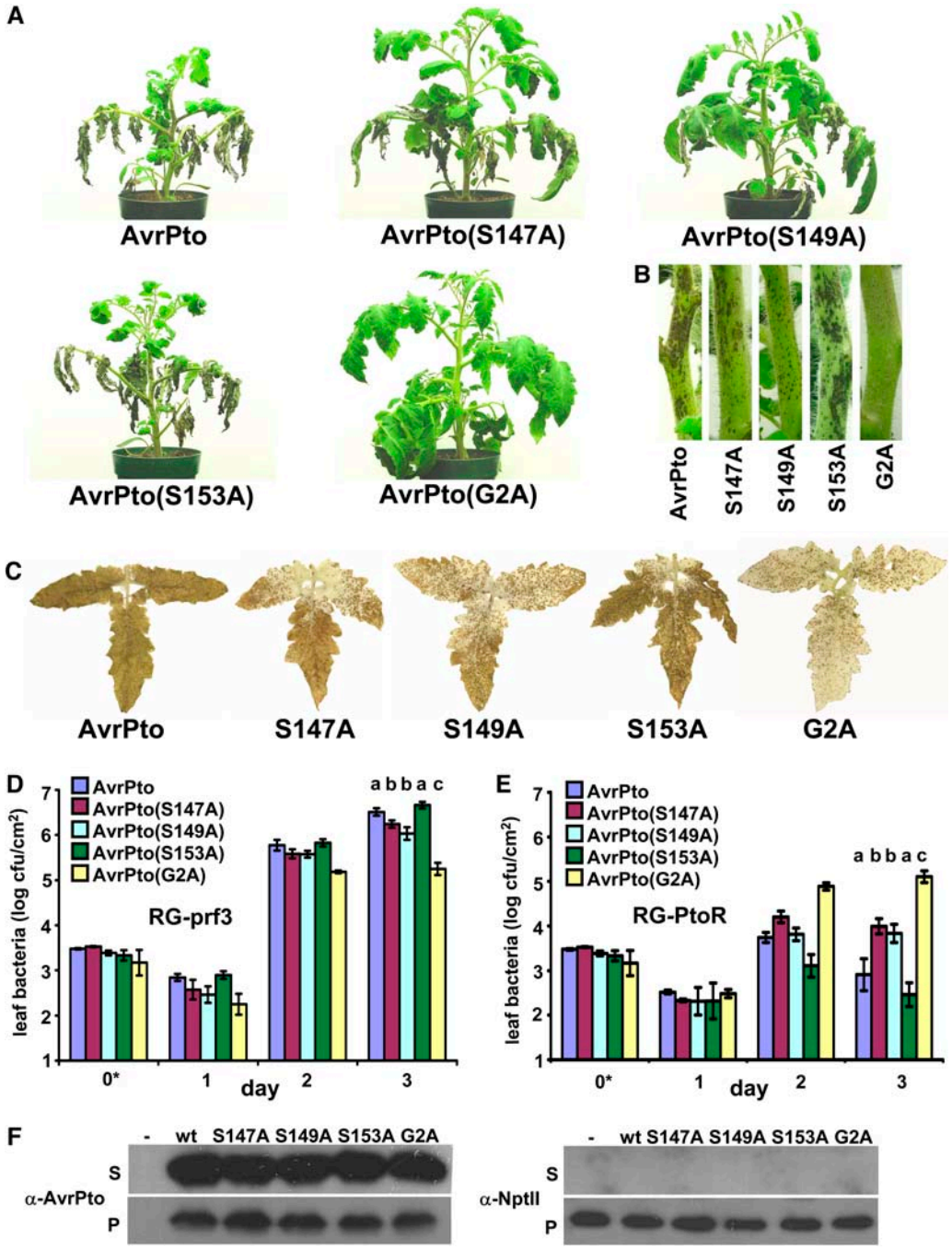


**Figure 7.** Phosphorylation Promotes Virulence and Avirulence Activity of AvrPto.

Ser-to-Ala mutants of AvrPto were introduced into *Pst* strain T1 on a broad host range vector to assess the function of phosphorylation in AvrPto virulence and avirulence activity in tomato.

**(A)** to **(C)** Disease symptoms observed on susceptible tomato RG-prf3 (*Pto*/*Pto prf*/*prf*) plants **(A)**, stems **(B)**, and leaflets **(C)**. Bacteria were inoculated at $10^4$ cfu/mL by vacuum infiltration. Photographs were taken 6 d after inoculation. Leaflets in **(C)** were removed and cleared of pigments 6 d after inoculation. Similar phenotypes of the mutants were observed in at least three independent experiments.

**(D)** Measurements of bacterial growth in leaves of RG-prf3 (*Pto*/*Pto prf*/*prf*). Data are in units of cfu per square centimeter of leaf tissue sampled. Graphed data are representative of two independent experiments ($n = 8$ for days 1, 2, and 3). Day 0* values for each strain are counts of bacteria plated from the inoculum prior to inoculation ($n = 3$). Letters above each mean represent groupings of statistical significance based on analysis of variance and pairwise Student's *t* test between strains on day 3 using Tukey's correction for multiple comparisons. $P \leq 0.05$ for all significant differences between strains. Error bars indicate $\pm$SE.

therefore do not appear to affect the stability or type III–dependent secretion of AvrPto.

## DISCUSSION

The functions of many type III effectors from phytopathogens remain unknown, in part due to the lack of sequence similarity between effectors and proteins of known function. In some cases, identifying posttranslational modifications of plant effectors has provided significant insights into their function (Mudgett and Staskawicz, 1999; Nimchuk et al., 2000). Yet, it is difficult to predict posttranslational modifications based on sequence analysis, and apart from proteolysis, most modifications are not easily detected by SDS-PAGE. To overcome these limitations, we developed a protocol using 2-D gel electrophoresis to identify modifications of an effector expressed in plant cells. Using this approach, we found evidence that AvrPto undergoes G2-dependent modifications (e.g., myristoylation) in plants (Figure 1). Furthermore, we found evidence that AvrPto is also phosphorylated (Figure 2). Both modifications occur as the result of interactions with two plant enzymes, an *N*-myristoyltransferase and a protein kinase, and enhance the virulence activity of AvrPto. These observations suggest that AvrPto has evolved to mimic host substrates to promote bacterial growth.

We performed experiments to characterize the host kinase(s) that phosphorylates AvrPto, to identify the phosphorylation sites on AvrPto, and to examine the biological implications of phosphorylation. Using an in vitro kinase assay, we found that recombinant AvrPto is phosphorylated by protein extracts from *N. benthamiana*, tobacco, tomato, and *Arabidopsis* leaves (Figure 3A). The presence of this activity in many plant species raises the possibility that AvrPto is a nonspecific substrate for many kinases in vitro. However, our results argue against this and suggest instead that AvrPto is a substrate for a specific host kinase activity. First, phosphorylation in vitro is limited to a small region at the C terminus of AvrPto, leaving a majority of potential sites on AvrPto unmodified (Figure 4). Second, extracts from all of the plant species tested in vitro phosphorylated the same Ser residues at the C terminus of AvrPto (Figure 5A). Third, gel filtration chromatography identified a single peak of kinase activity, suggesting that a specific host kinase or subset of host kinases may be involved (Figure 3B). Finally, we found a correlation between the phosphorylation sites we mapped in vitro and the in vivo phosphorylation sites of AvrPto observed by 2-D electrophoresis and mass spectrometry (Figure 5C). Together, these data indicate that a conserved plant kinase activity phosphorylates a discrete region of the C terminus of AvrPto.

Our mutagenesis and in vitro experiments identified three closely clustered Ser residues of AvrPto as possible phosphorylation sites, and our further analysis by mass spectrometry confirmed that one of these sites is phosphorylated in vivo in tomato. To determine if phosphorylation contributes to AvrPto virulence, we altered the confirmed phosphorylation site at S149 to Ala and examined the effects of this substitution on the growth of *Pst* in both susceptible and resistant tomato plants. We found that S149A decreases both the virulence and avirulence activity of AvrPto in tomato (Figure 7). In addition, an Ala substitution at S147 also decreases AvrPto activity in a similar manner. Given our inability to confirm S147 phosphorylation by mass spectrometry and the close proximity of S147 to S149, it is possible that the phenotypes observed with S147A may be caused by altering the kinase binding motif for S149. Alternatively, S147 may be an additional phosphorylation site that we have not detected in vivo. Nevertheless, our data provide a direct correlation between phosphorylation at S149 and decreased AvrPto virulence and avirulence activity. By contrast, an Ala substitution for S153 had no significant effect on AvrPto activity, although the trend observed in our data suggests that S153A may increase, rather than decrease, both virulence and avirulence. This result demonstrates that mutations made in the C terminus do not generally decrease AvrPto activity and argues that the loss of virulence/avirulence observed with S147A and S149A is specific to these residues. Our data also suggest that the phosphorylation site at S149 does not account for the full virulence activity of AvrPto in tomato. A separate study in our lab has identified additional structural determinants of AvrPto that contribute to virulence and may be responsible for the remaining S149-independent virulence activity observed in our assays (P.E. Pascuzzi and G.B. Martin, unpublished data).

Given the large number and diversity of effectors in bacterial plant pathogens, it is likely that other effectors from phytobacteria are substrates for host kinases. To investigate this possibility, we tested several other effectors as kinase substrates in vitro and found that AvrB from *P. syringae* is also strongly phosphorylated by tomato and tobacco leaf extracts (J.C. Anderson and G.B. Martin, unpublished data). Also, recent reports demonstrate that the type III effectors NopL and NopP from symbiotic *Rhizobium* sp strain NGR234 can be phosphorylated in vitro by plant extracts (Bartsev et al., 2004; Skorpil et al., 2005). Interestingly, expression of NopL in tobacco suppresses the activation of pathogenesis-related proteins due to viral infection, and NopP promotes root nodulation by *Rhizobium* (Bartsev et al., 2004; Skorpil et al., 2005). It remains to be determined if phosphorylation contributes to the phenotypes associated with NopL and NopP function. The identification and characterization of additional effectors that are phosphorylated would help determine if they are interacting with the same or different kinases and could provide useful insights into their function.

**Figure 7.** (continued).

**(E)** Measurements of bacterial growth in leaves of RG-PtoR (*Pto*/*Pto Prf*/*Prf*). Graphed data are representative of two independent experiments ($n = 6$ for days 1, 2, and 3). Day 0* values for each strain are counts of bacteria plated from the inoculum prior to inoculation as in **(D)** ($n = 3$). Details of statistical analysis are as in **(D)**. $P < 0.05$ for all significant differences between strains.

**(F)** Immunoblotting to confirm equal expression and secretion of AvrPto mutants from *Pst* T1 strains grown in minimal media under hrp-inducing conditions. Left panels are anti-AvrPto blots of supernatant (S) and pelleted (P) *Pst*, right panels are antineomycin phosphotransferase II ($\alpha$-NptII) blots to confirm that AvrPto in supernatant is not due to cell lysis.

There are several examples from mammalian pathogens where host-mediated phosphorylation contributes to the virulence activity of a type III effector. The translocated intimin receptor (Tir) from enteropathogenic *E. coli* is a type III–secreted protein that is phosphorylated after delivery into the host (Kenny et al., 1997; Warawa and Kenny, 2001). Phosphorylation of Tir is required for the binding of host proteins that, in turn, promote actin filament formation necessary for bacterial adhesion (Nougayrede et al., 2003). Another example is CagA, a type IV effector from *Helicobacter pylori* that is secreted directly into gastric epithelial cells and phosphorylated on Tyr residues by Src family kinases (Hatakeyama, 2004). Like AvrPto, CagA is associated with the host plasma membrane and is phosphorylated on its C terminus. Phosphorylation of CagA recruits the SHP-2 phosphatase, an interaction that promotes morphological changes in the host cell attributed to CagA virulence (Higashi et al., 2002). In this work, we demonstrate that the phosphorylated residues of AvrPto contribute to its virulence activity through an unknown molecular mechanism. We hypothesize that the phosphorylated C terminus of AvrPto could function in a manner similar to Tir and CagA by promoting interactions with proteins at the plasma membrane. It will be interesting to test if tomato AvrPto-interacting proteins identified in a yeast two-hybrid screen interact specifically with the C terminus and if this interaction is regulated by phosphorylation (Bogdanove and Martin, 2000).

Consistent with the observation that AvrPto localizes exclusively to the plasma membrane (Shan et al., 2000b), we found indirect evidence that suggests that AvrPto is myristoylated in plant cells (Figure 1). Posttranslational acylation is a virulence strategy that is thought to recruit host proteins to the plasma membrane or to promote interactions with membrane-bound proteins (Nimchuk et al., 2000). The virulence activity of AvrPto is dependent upon a functional myristoylation motif (Figure 6C; Thara et al., 2004). Interestingly, our 2-D data suggest that AvrPto is modified by phosphorylation independently of G2-dependent modifications in plant cells (Figure 1). Therefore, it appears that AvrPto must be localized to the plasma membrane in order for phosphorylation to promote virulence.

We present a model in Figure 8 to place our results in context with data from previous studies. The model highlights two structurally and functionally distinct regions of AvrPto: the $\alpha$-helical core containing the GINP loop and the unstructured C terminus. Mutational analyses have found that the GINP loop, namely residue I96, is strictly required for interacting with Pto in the yeast two-hybrid system and for eliciting Pto/Prf-mediated disease resistance (Shan et al., 2000a; Chang et al., 2001; Wulf et al., 2004). However, AvrPto still promotes significant *Pst* growth despite mutations in the GINP loop (Shan et al., 2000a). In this study, we find that phosphorylation of S149 at the C terminus of AvrPto promotes the enhanced disease symptoms and growth of *Pst* caused by AvrPto in tomato (Figure 7). In addition, we found that S149 phosphorylation contributes to the avirulence activity of AvrPto in resistant RG-PtoR plants (Figure 7E). Therefore, AvrPto appears to have two structurally distinct determinants, the GINP loop and the phosphorylation site at the C terminus, that influence either avirulence and/or virulence (Figure 8).

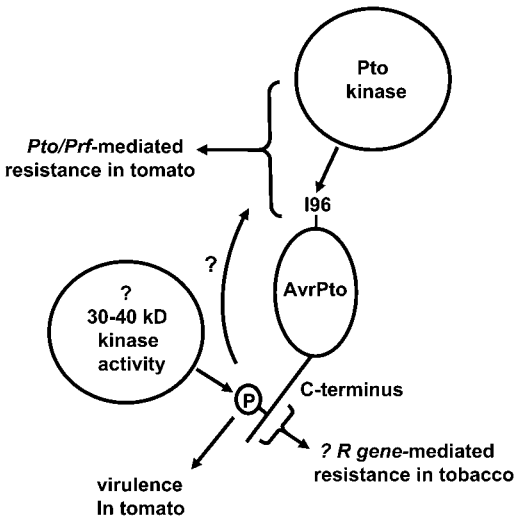


**Figure 8.** Model for Interaction between AvrPto and Two Distinct Host Kinases.

The structured $\alpha$-helical core of AvrPto is shown as a circle, and the C terminus is shown as a solid line. The Pto kinase interacts with the GINP loop of AvrPto designated by I96. A conserved 30- to 40-kD kinase activity phosphorylates S149 within the C terminus (indicated by the circled letter P). Our data demonstrate that phosphorylation of S149 contributes to the virulence and avirulence activity of AvrPto in tomato. Furthermore, the phosphorylated region of AvrPto is targeted for recognition in tobacco by an unknown *R* gene.

It is likely that R proteins evolved to recognize structural features of effectors that contribute to their virulence activity. Our results demonstrate that the phosphorylated C terminus of AvrPto promotes both virulence and avirulence activities of AvrPto in tomato (Figure 7). While the mechanism by which the C terminus contributes to avirulence is unclear, our data suggest that the C terminus virulence determinant of AvrPto is monitored by plant defenses. Further support for this co-dependence is provided by the discovery that the C terminus of AvrPto is recognized by an uncharacterized tobacco *R* gene (Shan et al., 2000b). Using random mutagenesis, Shan et al. (2000b) found that the mutations S153P, S147R, P146L, (P18Q, N145K), or (E138K, P146L) in AvrPto abolish recognition in tobacco. Interestingly, all of these mutations occurred at residues located near the phosphorylation site of AvrPto, including S147 and S153 (see sequence in Figure 5C). Despite this overlap, we have found that an AvrPto(S147A,S149A,S153A) mutant does not appear to affect the hypersensitive response elicited by AvrPto in tobacco when delivered by *P. s.* pv *tabaci* (J.C. Anderson and G.B. Martin, unpublished data). This observation indicates that structural features rather than phosphorylation per se may be required for recognition in tobacco. Nevertheless, the direct overlap between phosphorylation and recognition sites supports the prediction that plant R proteins target virulence determinants of effectors. We hypothesize that the interaction between AvrPto and the C terminus–specific kinase, rather than the phosphorylation state of AvrPto, might be important for recognition in tobacco.

Our discovery that AvrPto is modified by phosphorylation, and the subsequent functional analyses of the phosphorylation site we identified, has provided new insights about the structural determinants for AvrPto virulence activity in tomato. Interesting questions remain about how phosphorylated C terminus contributes to the function of this protein. Our research will focus on identifying the host kinase(s) involved and elucidating the molecular mechanism by which phosphorylation of AvrPto promotes *Pst* virulence.

## METHODS

### Plasmid Construction and Mutagenesis

For *Escherichia coli* expression, full-length or deletions of *avrPto* from *Pseudomonas syringae* pv *tomato* strain JL1065 were PCR amplified and subcloned into pFLAG-CTC (Sigma-Aldrich). The *35S*:*avrPto-dHA*:pCAMBIA vector for *Agrobacterium tumefaciens*–mediated expression has been described (He et al., 2004). A *35S*:*avrPto-HA*:pJD301 plasmid was used for protoplast expression. For *Pst* expression, a 750-bp fragment containing *avrPto* and promoter sequence was amplified from *Pst* strain JL1065 genomic DNA and then ligated into *KpnI*/*Xba*I sites of vector pDSK519. AvrPto mutations were created in appropriate plasmids using a site-directed mutagenesis kit (Stratagene).

### *Agrobacterium*-Mediated Expression of AvrPto and 2-D Gel Electrophoresis

*Agrobacterium* strain GV2260 was grown and infiltrated into *Nicotiana benthamiana* leaves as described (He et al., 2004). Five 1-cm-diameter leaf disks were isolated 24 h after infiltration of *Agrobacterium*, frozen in liquid $N_2$, and pulverized in 1 mL of extraction buffer (100 mM Tris-HCl, pH 7.5, 150 mM NaCl, 20 mM DTT, 1 mM EDTA, 1 mM phenylmethylsulfonyl fluoride, 5 μg/mL aprotinin, 5 μg/mL leupeptin, 0.1 mM NaVanadate, 10 mM NaF, 50 mM β-glycerophosphate, 1 mM EGTA, and 1% Triton X-100) using a glass homogenizer (Kontes) on ice. Extracts were spun at 16,000*g* for 15 min at 4°C and protein precipitated from 200 μL of supernatant using 4 volumes of ice-cold 12% trichloroacetic acid/20 mM DTT in acetone and incubation at −20°C. For phosphatase treatment, 200 μL of extract with 2 mM $MnCl_2$ (minus NaV and NaF) was incubated with ~2.5 μg of λ-PPase and 1.25 μg PP1 (New England Biolabs) with or without 5 mM NaVanadate and 10 μL phosphatase inhibitor cocktail I (Sigma-Aldrich) at 30°C for 20 min prior to precipitation. After 16,000*g* for 20 min, the pellet was washed with acetone and then resuspended in 300 μL of 7 M urea, 2 M thiourea, 60 mM DTT, 4% CHAPS, and 2% ampholytes. Immobiline Drystrips (13 cm; GE Healthcare) with a linear pH range of 3 to 10 were rehydrated with 250 μL of solubilized protein. Isoelectric focusing and SDS-PAGE were performed according to the manufacturer's protocol (GE Healthcare). For immunoblots, proteins were transferred to PVDF (Millipore). AvrPto was detected using rat anti-HA and goat anti-rat horseradish peroxidase (HRP)–conjugated antibodies (Roche) and an ECL kit (GE Healthcare).

### In Vivo $^{32}$P-Labeling of AvrPto

Protoplast isolation from tomato (*Solanum lycopersicum*) leaves and polyethylene glycol–mediated transfection are described elsewhere (Xing et al., 2001; http://genetics.mgh.harvard.edu/sheenweb/). Transfected protoplasts were incubated with 0.1 mCi/mL phosphorus-32 (GE Healthcare) for 8 h and lysed with PBS containing 0.5% Triton X-100, 0.5% EDTA, and phosphatase and plant protease inhibitors (Sigma-Aldrich). AvrPto was immunoprecipitated with anti-HA affinity matrix (Roche), followed by SDS-PAGE and autoradiography.

### In Vitro AvrPto Phosphorylation Assays

To prepare leaf protein extracts, 0.5 g of leaf tissue was ground in liquid $N_2$ and briefly vortexed in 5 mL of 25 mM Tris, pH 7.0, 50 mM NaCl, 10 mM EDTA, 5 mM DTT, 20% sucrose, and 25 μL plant protease inhibitor (Sigma-Aldrich). The extract was spun at 8,000*g* for 5 min and the supernatant strained through MiraCloth (Calbiochem). Proteins were precipitated by addition of $(NH_4)_2S0_4$ to 50% (w/v), mixed for 2 h, and pelleted by 8,000*g* for 10 min. Proteins were resuspended and dialyzed into 20 mM Tris-HCl, pH 7.5, 50 mM NaCl, 1 mM DTT, and 10% glycerol. AvrPto-FLAG was expressed in and purified from *E. coli* as described previously using anti-FLAG resin (Sigma-Aldrich; Wulf et al., 2004). For a typical assay, 20 μL of resin with AvrPto bound (~2 μg) was incubated with 10 μL of leaf extract (~5 μg) in 70 μL of TBS buffer with 1 mM $MgCl_2$, 20 μM ATP, and 10 μCi [γ-$^{32}$P]ATP for 10 min at 25°C. Reactions were stopped and washed with TBS buffer containing 50 mM EDTA and separated by SDS-PAGE. $^{32}$P-labeling of AvrPto was detected by a phosphor imager (GE Healthcare). AvrPto-FLAG was detected by rabbit anti-FLAG (Sigma-Aldrich) and HRP-conjugated anti-rabbit (Promega). For gel filtration, tomato or tobacco (*Nicotiana tabacum*) leaf extracts were prepared as above, separated using a Superdex 200 column (GE Healthcare), and calibrated with molecular weight standards (Bio-Rad).

### Phosphoamino Acid Analysis

$^{32}$P-labeled AvrPto was hydrolyzed to its constituent amino acids and separated by thin layer chromatography using methods described previously (Van der Geer et al., 1993).

### nanoESI-MS/MS Identification of AvrPto Phosphorylation Sites

Tomato protoplasts were isolated and transformed with plasmid pJD301 expressing AvrPto-dHA or AvrPto(ΔC30) under the *35S* promoter control as described above. A total of $1.5 \times 10^6$ protoplasts were transformed (six aliquots of $2.5 \times 10^5$ protoplasts each transformed with 20 μg DNA) for each construct and incubated for 24 h. Following incubation, the transformed protoplasts for each construct were pooled, sedimented by centrifugation, and lysed in 6 mL of 50 mM Tris, pH 7.5, 50 mM NaCl, 10 mM EDTA, 1% Triton X-100, and 10 μL/mL plant protease and phosphatase inhibitor I cocktails (Sigma-Aldrich). Rat anti-HA IgG (10 μg) and 50 μL protein G-agarose beads (Roche) were added and the lysates incubated at 4°C for 2 h with shaking. The agarose beads were then sedimented and washed extensively in 50 mM Tris, pH 7.5, 150 mM NaCl, 10 mM EDTA, and 1% Triton X-100 and resuspended in Laemmli buffer. Proteins were separated on 15% SDS-PAGE gels and detected by Coomassie Brilliant Blue G 250. Mass spectrometry was performed at the Proteomics and Mass Spectrometry Facility (Donald Danforth Plant Science Center, St. Louis, MO). Bands corresponding to AvrPto and AvrPto(ΔC30) were subjected to in-gel digestion as previously described (Gabelica et al., 2002), except digestion was conducted at 37°C for 10 h in 50 mM $NH_4HCO_3$ containing 6 μg/mL modified trypsin (Promega), and then a double extraction was performed, first with 1% formic acid/2% acetonitrile and second with 60% acetonitrile. The pooled digest was lyophilized and resuspended into 1% formic acid/2% acetonitrile followed by $ZipTip_{\mu C18}$ (Millipore) sample cleanup according to the manufacturer's instructions and eluted into 0.1% formic acid/60% acetonitrile. An ABI QSTAR XL hybrid quadrupole time-of-flight MS/MS system (Applied Biosystems/MDS Sciex) equipped with a nano-electrospray source was used for peptide sequence analysis. Time-of-flight MS spectra and product ion spectra were acquired using information-dependent data acquisition in the Analyst QS software (Applied Biosystems). Peptide identification and assignment of partial posttranslational modifications were performed using an in-house version of Mascot version 1.9 (Perkins et al., 1999). All data sets were searched against NCBInr using the following constraints: only tryptic

peptides with up to one missed cleavage site were allowed; 1.0 and 0.1 D mass tolerances for MS and MS/MS fragment ions. The charge states of precursor ions selected were 2 to 4. Phosphorylation (Ser/Thr/Tyr) and oxidation (Met) were specified as variable modifications. The MS/MS spectra were inspected for neutral loss, sequence-specific fragmentation patterns, and database match. The Mascot search results calculated all hits with a score above 55 to be significant ($P < 0.05$). Unambiguous identification of a phosphorylation site was made by the quality of MS/MS spectra and the scores for peptide without and with phosphate at different positions.

### *Pst* T1 Growth Assays

Transconjugates of *Pst* T1 carrying AvrPto:PDSK519 plasmids were obtained using triparental mating. Prior to inoculation, T1 strains were streaked from glycerol stocks onto King's B (KB) medium plates containing rifampicin (100 mg/L) and kanamycin (25 mg/L) and incubated at 30°C for 3 d. To ensure consistent growth between strains taken from glycerol stocks, a small amount of each strain was then resuspended in liquid KB medium to an $OD_{600}$ of 0.1, and 0.1 mL of this suspension spotted onto a fresh KB plate as above and incubated for 2 d at 25°C. These cells were resuspended in 0.1 M sucrose containing 10 mM $MgCl_2$ to an $OD_{600}$ of 0.1. This was used to inoculate 4 liters of 10 mM $MgCl_2$ containing 0.002% Silwet to a final $OD_{600}$ of $5 \times 10^{-5}$. Day 0 counts were obtained by plating 10-fold dilution of three samples from each inoculum on KB medium plates and counting the resulting colonies.

Tomato plants used for the assays were transplanted to 4-inch pots 1 to 2 weeks before infiltration and moved to a climate-controlled growth chamber that was maintained at 24°C during the day and 20°C at night, with 75% humidity and 16-h days. Plants were infiltrated 4 weeks after seed sowing by totally immersing the plants in the inoculum and subjecting them to a 2-min vacuum with a pump rated at 10 torr and 29.3 L/min. After air-drying, plants were returned to the growth chamber. Bacterial growth was monitored over several days with samples taken on days 1, 2, and 3. Methods for counting bacteria were adapted from a previously described protocol (Tornero and Dangl, 2001). Each sample consisted of three 1-cm-diameter discs taken from one leaflet, with two leaves sampled per plant. Discs were floated abaxial side down on 1 mL of 0.1 M sucrose containing 10 mM $MgCl_2$ and incubated at 12°C and 125 rpm for 4 h. Five- or 10-fold serial dilutions were made, and 10 μL of these dilutions were spotted onto KB plates with antibiotics as above. Both the dilutions and subsequent plating were done using a Genesis RSP 200 liquid handling system (Tecan). Colonies were counted 48 to 60 h after plating with the aid of a dissecting microscope. Tomato leaves were destained using Carnoy's fluid (10% acetic acid, 30% chloroform, and 60% ethanol). We have found consistent handling of bacterial strains and plants as well as the use of a climate-controlled growth chamber to be critical factors in producing consistent and reproducible results. Protocols used for *Pst* expression and secretion of AvrPto in minimal media have been described (Shan et al., 2000b). Immunoblotting was performed with anti-AvrPto (Shan et al., 2000a) and rabbit anti-NptII (US Biological).

### Accession Number

Sequence data from this article can be found in the GenBank/EMBL data library under accession number L20425.

### Supplemental Data

The following material is available in the online version of this article.

**Supplemental Figure 1.** Subcellular Fractionation of AvrPto Kinase Activity in Leaf Protein Extracts.

## ACKNOWLEDGMENTS

We thank Sixue Chen for performing the mass spectrometry and Fred McLafferty and Jocelyn Rose for evaluation of our mass spectrometry results. We thank Mark D'Ascenzo for assistance with phosphoamino acid analysis and the Boyce Thompson Institute greenhouse staff for plant care. For critical reading of the manuscript, we thank Jonathan Cohn, Peter Moffett, Robert Abramovitch, and Patrick Giavalisco. This work was supported by Grants USDA-NRI-2002-01235 and USDA-NRI-2005-00972 (G.B.M.), by the Triad Foundation (G.B.M.), and by Binational Science Foundation 2001124 (G.B.M. and G.S.).

Received July 28, 2005; revised November 29, 2005; accepted December 12, 2005; published January 6, 2006.

## REFERENCES

**Alfano, J.R., and Collmer, A.** (2004). Type III secretion system effector proteins: Double agents in bacterial disease and plant defense. Annu. Rev. Phytopathol. **42,** 385–414.

**Bartsev, A.V., Deakin, W.J., Boukli, N.M., McAlvin, C.B., Stacey, G., Malnoe, P., Broughton, W.J., and Staehelin, C.** (2004). NopL, an effector protein of *Rhizobium* sp. NGR234, thwarts activation of plant defense reactions. Plant Physiol. **134,** 871–879.

**Bogdanove, A.J., and Martin, G.B.** (2000). AvrPto-dependent Pto-interacting proteins and AvrPto-interacting proteins in tomato. Proc. Natl. Acad. Sci. USA **97,** 8836–8840.

**Bretz, J.R., Mock, N.M., Charity, J.C., Zeyad, S., Baker, C.J., and Hutcheson, S.W.** (2003). A translocated protein tyrosine phosphatase of *Pseudomonas syringae* pv. *tomato* DC3000 modulates plant defence response to infection. Mol. Microbiol. **49,** 389–400.

**Buttner, D., and Bonas, U.** (2003). Common infection strategies of plant and animal pathogenic bacteria. Curr. Opin. Plant Biol. **6,** 312–319.

**Chang, J.H., Rathjen, J.P., Bernal, A.J., Staskawicz, B.J., and Michelmore, R.W.** (2000). AvrPto enhances growth and necrosis caused by *Pseudomonas syringae* pv. *tomato* in tomato lines lacking either *Pto* or *Prf.* Mol. Plant Microbe Interact. **13,** 568–571.

**Chang, J.H., Tobias, C.M., Staskawicz, B.J., and Michelmore, R.W.** (2001). Functional studies of the bacterial avirulence protein AvrPto by mutational analysis. Mol. Plant Microbe Interact. **14,** 451–459.

**Coaker, G., Falick, A., and Staskawicz, B.J.** (2005). Activation of a phytopathogenic bacterial effector protein by a eukaryotic cyclophilin. Science **308,** 548–550.

**Collmer, A., Lindeberg, M., Petnicki-Ocwieja, T., Schneider, D.J., and Alfano, J.R.** (2002). Genomic mining type III secretion system effectors in *Pseudomonas syringae* yields new picks for all TTSS prospectors. Trends Microbiol. **10,** 462–469.

**Espinosa, A., Guo, M., Tam, V.C., Fu, Z.Q., and Alfano, J.R.** (2003). The *Pseudomonas syringae* type III-secreted protein HopPtoD2 possesses protein tyrosine phosphatase activity and suppresses programmed cell death in plants. Mol. Microbiol. **49,** 377–387.

**Gabelica, V., Vreuls, C., Filee, P., Duval, V., Joris, B., and Pauw, E.D.** (2002). Advantages and drawbacks of nanospray for studying non-covalent protein-DNA complexes by mass spectrometry. Rapid Commun. Mass Spectrom. **16,** 1723–1728.

**Garcia, B.A., Shabanowitz, J., and Hunt, D.F.** (2005). Analysis of protein phosphorylation by mass spectrometry. Methods **35,** 256–264.

**Guan, K.L., and Dixon, J.E.** (1990). Protein tyrosine phosphatase activity of an essential virulence determinant in *Yersinia.* Science **249,** 553–556.

**Hatakeyama, M.** (2004). Oncogenic mechanisms of the *Helicobacter pylori* CagA protein. Nat. Rev. Cancer **4,** 688–694.

**Hauck, P., Thilmony, R., and He, S.Y.** (2003). A *Pseudomonas syringae* type III effector suppresses cell wall-based extracellular defense in susceptible *Arabidopsis* plants. Proc. Natl. Acad. Sci. USA **100,** 8577–8582.

**He, X., Anderson, J.C., del Pozo, O., Gu, Y.-Q., Tang, X., and Martin, G.B.** (2004). Silencing of subfamily I of protein phosphatase 2A catalytic subunits results in activation of plant defense responses and localized cell death. Plant J. **38,** 563–577.

**Higashi, H., Tsutsumi, R., Muto, S., Sugiyama, T., Azuma, T., Asaka, M., and Hatakeyama, M.** (2002). SHP-2 tyrosine phosphatase as an intracellular target of *Helicobacter pylori* CagA protein. Science **295,** 683–686.

**Kang, L., Tang, X., and Mysore, K.S.** (2004). *Pseudomonas* Type III effector AvrPto suppresses the programmed cell death induced by two nonhost pathogens in *Nicotiana benthamiana* and tomato. Mol. Plant Microbe Interact. **17,** 1328–1336.

**Kenny, B., DeVinney, R., Stein, M., Reinscheid, D.J., Frey, E.A., and Finlay, B.B.** (1997). Enteropathogenic *E. coli* (EPEC) transfers its receptor for intimate adherence into mammalian cells. Cell **91,** 511–520.

**Kim, H.-S., Desveaux, D., Singer, A.U., Patel, P., Sondek, J., and Dangl, J.L.** (2005). The *Pseudomonas syringae* effector AvrRpt2 cleaves its C-terminally acylated target, RIN4, from *Arabidopsis* membranes to block RPM1 activation. Proc. Natl. Acad. Sci. USA **102,** 6496–6501.

**Kubori, T., and Galan, J.E.** (2003). Temporal regulation of *Salmonella* virulence effector function by proteasome-dependent protein degradation. Cell **115,** 333–342.

**Marcus, S.L., Knodler, L.A., and Finlay, B.B.** (2002). *Salmonella enterica* serovar *typhimurium* effector SigD/SopB is membrane-associated and ubiquitinated inside host cells. Cell. Microbiol. **4,** 435–446.

**Martin, G.B., Bogdanove, A.J., and Sessa, G.** (2003). Understanding the functions of plant disease resistance proteins. Annu. Rev. Plant Biol. **54,** 23–61.

**McDonald, C., Vacratsis, P.O., Bliska, J.B., and Dixon, J.E.** (2003). The *Yersinia* virulence factor YopM forms a novel protein complex with two cellular kinases. J. Biol. Chem. **278,** 18514–18523.

**Mudgett, M.B., and Staskawicz, B.J.** (1999). Characterization of the *Pseudomonas syringae* pv. *tomato* AvrRpt2 protein: Demonstration of secretion and processing during bacterial pathogenesis. Mol. Microbiol. **32,** 927–941.

**Navarro, L., Alto, N.M., and Dixon, J.E.** (2005). Functions of the *Yersinia* effector proteins in inhibiting host immune responses. Curr Opin. Microbiol. **8,** 21–27.

**Nimchuk, Z., Marois, E., Kjemtrup, S., Leister, R.T., Katagiri, F., and Dangl, J.L.** (2000). Eukaryotic fatty acylation drives plasma membrane targeting and enhances function of several type III effector proteins from *Pseudomonas syringae.* Cell **101,** 353–363.

**Nougayrede, J.P., Fernandes, P.J., and Donnenberg, M.S.** (2003). Adhesion of enteropathogenic *Escherichia coli* to host cells. Cell. Microbiol. **5,** 359–372.

**Orth, K., Palmer, L.E., Bao, Z.Q., Stewart, S., Rudolph, A.E., Bliska, J.B., and Dixon, J.E.** (1999). Inhibition of the mitogen-activated protein kinase kinase superfamily by a *Yersinia* effector. Science **285,** 1920–1923.

**Pedley, K.F., and Martin, G.B.** (2003). Molecular basis of Pto-mediated resistance to bacterial speck disease. Annu. Rev. Phytopathol. **41,** 215–243.

**Perkins, D.N., Pappin, D.J.C., Creasy, D.M., and Cottrell, J.S.** (1999). Probability-based protein identification by searching sequence databases using mass spectrometry data. Electrophoresis **20,** 3551–3567.

**Salmeron, J.M., Oldroyd, G.E.D., Rommens, C.M.T., Scofield, S.R., Kim, H.-S., Lavelle, D.T., Dahlbeck, D., and Staskawicz, B.J.** (1996). Tomato *Prf* is a member of the leucine-rich repeat class of plant disease resistance genes and lies embedded within the *Pto* kinase gene cluster. Cell **86,** 123–133.

**Scofield, S.R., Tobias, C.M., Rathjen, J.P., Chang, J.H., Lavelle, D.T., Michelmore, R.W., and Staskawicz, B.J.** (1996). Molecular basis of gene-for-gene specificity in bacterial speck disease of tomato. Science **274,** 2063–2065.

**Shan, L., He, P., Zhou, J.M., and Tang, X.** (2000a). A cluster of mutations disrupt the avirulence but not the virulence function of AvrPto. Mol. Plant Microbe Interact. **13,** 592–598.

**Shan, L., Thara, V.K., Martin, G.B., Zhou, J.-M., and Tang, X.** (2000b). The *Pseudomonas* AvrPto protein is differentially recognized by tomato and tobacco and is localized to the plant plasma membrane. Plant Cell **12,** 2323–2338.

**Shao, F., Golstein, C., Ade, J., Stoutemyer, M., Dixon, J.E., and Innes, R.W.** (2003). Cleavage of *Arabidopsis* PBS1 by a bacterial type III effector. Science **301,** 1230–1233.

**Skorpil, P., Saad, M.M., Boukli, N.M., Kobayashi, H., Ares-Orpel, F., Broughton, W.J., and Deakin, W.J.** (2005). NopP, a phosphorylated effector of Rhizobium sp. strain NGR234, is a major determinant of nodulation of the tropical legumes *Flemingia congesta* and *Tephrosia vogelii.* Mol. Microbiol. **57,** 1304–1317.

**Stebbins, C.E., and Galan, J.E.** (2001). Structural mimicry in bacterial virulence. Nature **412,** 701–705.

**Tang, X., Frederick, R.D., Zhou, J., Halterman, D.A., Jia, Y., and Martin, G.B.** (1996). Initiation of plant disease resistance by physical interaction of AvrPto and Pto kinase. Science **274,** 2060–2063.

**Thara, V.K., Seilaniantz, Y., Deng, Y., Dong, Y., Yang, X., Tang, X., and Zhou, J.M.** (2004). Tobacco genes induced by the bacterial effector protein AvrPto. Mol. Plant Microbe Interact. **17,** 1139–1145.

**Tornero, P., and Dangl, J.L.** (2001). A high-throughput method for quantifying growth of phytopathogenic bacteria in *Arabidopsis thaliana.* Plant J. **28,** 475–481.

**Van der Geer, P., Luo, K., Sefton, B.M., and Hunter, T.** (1993). Phosphopeptide mapping and phosphoamino acid analysis on cellulose thin-layer plates. In Protein Phosphorylation: A Practical Approach, D.G. Hardie, ed (Oxford: IRL Press at Oxford University Press), pp. 31–59.

**Warawa, J., and Kenny, B.** (2001). Phosphoserine modification of the enteropathogenic *Escherichia coli* Tir molecule is required to trigger conformational changes in Tir and efficient pedestal elongation. Mol. Microbiol. **42,** 1269–1280.

**Wulf, J., Pascuzzi, P.E., Fahmy, A., Martin, G.B., and Nicholson, L.K.** (2004). The solution structure of type III effector protein AvrPto reveals conformational and dynamic features important for plant pathogenesis. Structure **12,** 1257–1268.

**Xing, T., Malik, K., Martin, T., and Miki, B.L.** (2001). Activation of tomato PR and wound-related genes by a mutagenized tomato MAP kinase kinase through divergent pathways. Plant Mol. Biol. **46,** 109–120.

# Host-Mediated Phosphorylation of Type III Effector AvrPto Promotes *Pseudomonas* Virulence and Avirulence in Tomato

Jeffrey C. Anderson, Pete E. Pascuzzi, Fangming Xiao, Guido Sessa and Gregory B. Martin

*Plant Cell* 2006;18;502-514; originally published online January 6, 2006;
DOI 10.1105/tpc.105.036590